Classical Origins of Landau-Incompatible Transitions

Abhishodh Prakash[1,2,*] and Nick G. Jones[3,†]

[1]*Rudolf Peierls Centre for Theoretical Physics, University of Oxford, United Kingdom*
[2]*Harish-Chandra Research Institute, Prayagraj (Allahabad), India*
[3]*St John's College and Mathematical Institute, University of Oxford, United Kingdom*

(Received 15 June 2024; accepted 12 February 2025; published 6 March 2025)

Continuous phase transitions where symmetry is spontaneously broken are ubiquitous in physics and often found between "Landau-compatible" phases where residual symmetries of one phase are a subset of the other. However, continuous "deconfined quantum critical" transitions between Landau-incompatible symmetry-breaking phases are known to exist in certain quantum systems, often with anomalous microscopic symmetries. In this Letter, we investigate the need for such special conditions. We show that Landau-incompatible transitions can be found in a family of well-known classical statistical mechanical models with anomaly-free symmetries, introduced by José *et al.* [Phys. Rev. B **16**, 1217 (1977).]. The models are anisotropic deformations of the classical 2D XY model labeled by a positive integer Q. For a range of temperatures, even Q models exhibit two Landau-incompatible partial symmetry-breaking phases and a direct transition between them for $Q \geq 4$. Characteristic features of deconfined quantum criticality, such as enhanced symmetries and melting of charged defects, are easily seen in a classical setting. For odd Q and corresponding temperature ranges, two regions of a single partial symmetry-breaking phase appear, split by a stable "unnecessary critical" line. We discuss experimental systems that realize these transitions and present anomaly-free quantum models that also exhibit similar phase diagrams.

DOI: 10.1103/PhysRevLett.134.097103

Spontaneous symmetry breaking (SSB) underpins several important physical phenomena, from the development of long-range orders in matter to endowing mass to fundamental particles [1]. The simplest setting for SSB is when a phase of matter, classical or quantum, with a vacuum invariant under a symmetry group G, undergoes a phase transition to produce multiple vacua, each of which preserves only a subset of the original symmetries $H \subset G$. If such a phase transition is continuous, it can be described within the Landau-Ginzburg-Wilson-Fisher (LGWF) framework using a local order parameter field. About 20 years ago, the nature of exotic direct transitions between incompatible SSB quantum phases, where the vacuum symmetries of neither phase could be identified as a subset of the other, was investigated in two-dimensional quantum systems [2]. Although such transitions had appeared in earlier studies [3], Ref. [2] recognized that they could not be framed within the LGWF paradigm in terms of order parameter fields. Instead, they were naturally formulated using gauge fields, which are hidden from sight in the ordered phases but appear at the transition. This prompted the moniker "deconfined quantum criticality" (DQC) [2,4].

What physical settings can give rise to such Landau-incompatible transitions? Low-dimensional examples [5–8] and descriptions using nonlinear sigma models [9] have clarified that deconfined gauge fields are not essential. However, quantum effects are believed to play a necessary role in DQC [10], especially when viewed from the role played by Berry phases, and most examples of DQC occur under Lieb-Schultz-Mattis conditions [3], when microscopic symmetries are *anomalous* [11,12].

In this Letter, we show that these conditions are *not* necessary and Landau-incompatible transitions can, in fact, be found even in ordinary classical statistical mechanical systems with anomaly-free symmetries. We demonstrate this using a well-known family of models introduced by José, Kadanoff, Kirkpatrick, and Nelson (JKKN) [13] obtained by perturbing the 2D classical XY model by on-site anisotropies labeled by a positive integer Q. For even $Q \geq 4$, the phase diagram includes a direct phase transition between two Landau-incompatible partial symmetry-breaking phases. This transition displays all notable characteristics of DQC, including the appearance of an enhanced symmetry that rotates between the order

*Contact author: abhishodh.prakash@physics.ox.ac.uk (he/him/his)
†Contact author: nick.jones@maths.ox.ac.uk

parameters of the Landau-incompatible phases and the melting of charged defects. Interestingly, neutral defects and isolated charges also independently exist and can condense to produce Landau-compatible phase transitions. For odd Q, we find an exotic second-order "unnecessary critical" line separating two regions of single phase that does not represent a genuine phase transition [14,15] but is nevertheless stable. To our knowledge, this is the first case of unnecessary criticality identified in a classical model. We discuss experimental systems that exhibit these phenomena and also present a family of quantum models with anomaly-free symmetries that exhibit similar phase diagrams. Our results show that exotic transitions beyond the LGWF paradigm are more abundant than previously believed.

Models and phase diagram—Let us consider the JKKN model [13], a classical statistical mechanical system of planar rotors $\theta_j \sim \theta_j + 2\pi$ located on the vertices of any two-dimensional lattice. The Hamiltonian is

$$H = -\sum_{\langle j,k \rangle} \cos(\theta_j - \theta_k) - \sum_{\ell=1,2,\ldots} \gamma_\ell \sum_j \cos(\ell Q \theta_j). \qquad (1)$$

Here, j labels the vertices and $\langle j,k \rangle$ the edges of the lattice. The relevant symmetry group of the system is generated by a rotation $\mathcal{R}$ and a reflection $\mathcal{T}$ acting as

$$\mathcal{R}\colon\ \theta_j \mapsto \theta_j + 2\pi/Q, \qquad \mathcal{T}\colon\ \theta_j \mapsto -\theta_j. \qquad (2)$$

The two generators do not commute but satisfy

$$\mathcal{T}\mathcal{R} = \mathcal{R}^{-1}\mathcal{T}, \qquad \mathcal{R}^Q = \mathcal{T}^2 = 1, \qquad (3)$$

and form the non-Abelian dihedral group $D_{2Q} \cong \mathbb{Z}_Q \rtimes \mathbb{Z}_2$. We will be interested in the equilibrium phase diagram of Eq. (1), varying the temperature $T = \beta^{-1}$ and γ_1 close to $\gamma_1 = 0$, while keeping all other couplings fixed, the most important being γ_2. This is shown schematically in Fig. 1 for $\gamma_2 < 0$ and all $|\gamma_\ell|$ kept small [16]. Let us summarize its main aspects [13,32]. (1) At low temperatures and $\gamma_2 < 0$, we obtain an ordered phase with full symmetry breaking and $2Q$ vacua (abbreviated f-SSB). For $\gamma_2 > 0$, this becomes a first-order line separating partial SSB regions described below [16]. (2) For a range of intermediate temperatures, we obtain two regions with partial SSB (abbreviated p-SSB$_\pm$ for $\gamma_1 > 0$ and $\gamma_1 < 0$, respectively), each containing Q vacua. These are separated from the f-SSB phase by an Ising transition for any Q [33]. For even Q, p-SSB$_\pm$ represent two distinct Landau-incompatible SSB phases, whereas for odd Q, they correspond to the same phase. (3) For $Q \geq 3$, the two partial SSB regions are separated by a critical line at $\gamma_1 = 0$, which is of prime interest. For even Q, this is a direct, stable Landau-incompatible transition. For odd Q, this line represents "unnecessary criticality" [14,15] and is expected to terminate under appropriate strong perturbation. (4) At high temperatures, we get a disordered paramagnetic phase (PM) that restores all symmetries. This is separated from the partial SSB phases by a direct transition belonging to the Ising, 3-state Potts, and Ashkin-Teller universality classes (or their symmetry-enriched variants [16,34,35]) for $Q = 2, 3, 4$, respectively [32], and by an intermediate gapless phase for $Q \geq 5$ [13].

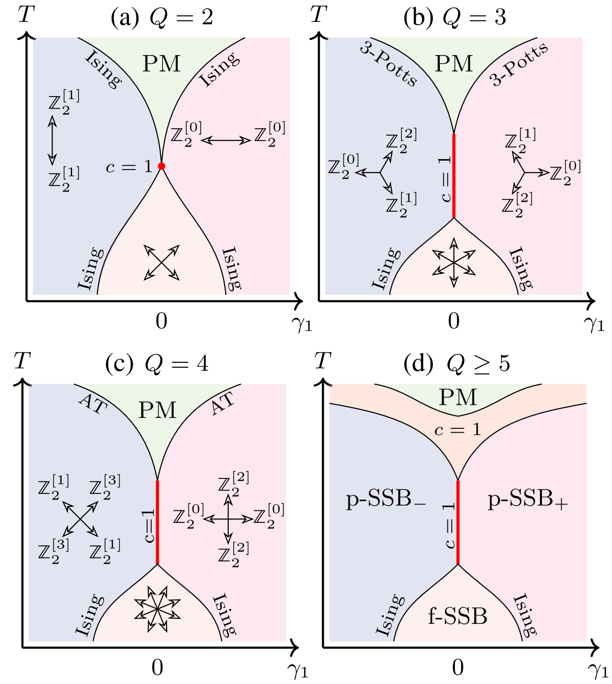

FIG. 1. Phase diagrams for the JKKN Hamiltonian shown in Eq. [1] for (a) $Q = 2$, (b) $Q = 3$, (c) $Q = 4$, (d) $Q \geq 5$, and for fixed $\gamma_2 < 0$. The arrows represent the different vacua characterized by the expectation value $\langle \theta_j \rangle$. The residual symmetry for each vacuum is shown following the notation in Eq. (8). For even $Q \geq 4$, the red line along $\gamma_1 = 0$ represents a direct transition between Landau-incompatible partial symmetry-breaking (p-SSB) phases. For odd $Q \geq 3$, it represents an unnecessary critical transition. The labels Ising, Ashkin-Teller (AT), 3-state Potts, and compact boson ($c = 1$) indicate the conformal field theory describing the transition. At high temperatures we have a paramagnetic (PM) phase.

The phase diagrams in Fig. 1 are determined by replacing Eq. (1) by an effective Gaussian continuum theory [13,32] via a duality transformation á la Villain [36],

$$S \approx \int d^2x \left[\frac{(\nabla\phi)^2}{8\pi^2\beta} - h\cos(\phi) - \sum_\ell \gamma_\ell \cos(\ell Q \theta) \right], \qquad (4)$$

and keeping track of the relevance (in the renormalization group sense) of the scaling operators $\cos(\phi)$ and $\cos(\ell Q \theta)$ [13,16]. Recall that a scaling operator $\mathcal{O}$ is relevant when its scaling dimension $[\mathcal{O}]$ is smaller than the spatial dimension (two in our case) for such classical statistical mechanical systems [37]. The term $h\cos(\phi)$ is included as a regulator in the Villain procedure. Close to the fixed point that is described by conformal field theory, the scaling dimensions are determined by a single stiffness parameter $K_{\rm eff}$ as [13,16,38]

$$[\cos(\phi)] = \pi K_{\rm eff}, \qquad [\cos(\ell Q\theta)] = \frac{\ell^2 Q^2}{4\pi K_{\rm eff}}. \quad (5)$$

While the exact relationship between $K_{\rm eff}$ and the microscopic parameters T, h, γ_ℓ cannot be determined exactly, we see that for $Q \geq 4$, there exists a regime $Q^2/(8\pi) < K_{\rm eff} < Q^2/(2\pi)$ where $\cos(Q\theta)$ is the only relevant symmetry-allowed operator. Tuning this away by setting $\gamma_1 = 0$ produces a critical state corresponding to the Landau-incompatible transition or unnecessary critical line. Important parts of the phase diagrams in Fig. 1 have already been explored in previous work (see Refs. [13,32]). Our main focus will be on symmetry properties, the Landau-compatible (incompatible) nature of transitions, unnecessary criticality, and the distinction between even and odd Q. These aspects have not been investigated previously, to the best of our knowledge.

Residual symmetries, Landau (in)compatibility—Let us understand the nature of the partial symmetry breaking regions (p-SSB$_\pm$) that are realized for $\gamma_1 > 0$ and $\gamma_1 < 0$, respectively, at intermediate temperatures, where the only relevant operator in Eq. (4) is $\cos(Q\theta)$. Both have Q vacua $\vartheta_1^\pm, \ldots, \vartheta_Q^\pm$ characterized by the vacuum expectation value $\langle\theta_j\rangle = \vartheta_n^\pm$ with

$$\vartheta_n^+ = 2\pi n/Q, \qquad \vartheta_n^- = (2n+1)\pi/Q. \quad (6)$$

The symmetries shown in Eq. (2) act on the vacua as

$$\mathcal{R}\colon \vartheta_n^\pm \mapsto \vartheta_{n+1}^\pm, \qquad \mathcal{T}\colon \begin{pmatrix} \vartheta_n^+ \\ \vartheta_n^- \end{pmatrix} \mapsto \begin{pmatrix} \vartheta_{-n}^+ \\ \vartheta_{-n-1}^- \end{pmatrix}. \quad (7)$$

Since both regions have the same number of vacua, only two possibilities exist: (i) the regions are distinct phases that are Landau-incompatible or (ii) they correspond to the same phase. To clarify which, we need to determine the residual symmetries of each vacuum, $\mathcal{I}(\vartheta_n^\pm)$, in both regions. Using Eq. (7), we see that the vacua transform into each other under the discrete rotations $\mathcal{R}$ but preserve a specific $\mathbb{Z}_2$ subgroup generated by reflection $\mathcal{T}$ followed by a certain number of rotations $\mathcal{R}$. To distinguish between various $\mathbb{Z}_2$ groups, we define the following notation:

$$\mathbb{Z}_2^{[\alpha]} \equiv \{1, \mathcal{R}^\alpha \mathcal{T}\} \quad (8)$$

with $\alpha = \alpha + Q$ identified. Using these, we get

$$\mathcal{I}(\vartheta_n^+) = \mathbb{Z}_2^{[2n]}, \quad \mathcal{I}(\vartheta_n^-) = \mathbb{Z}_2^{[2n+1]}, \quad \text{for } n = 0, \ldots, Q-1. \quad (9)$$

Figure 1 shows the residual symmetries for $Q = 2, 3, 4$. For even Q, these are distinct for p-SSB$_\pm$ and the vacua are invariant under $\mathcal{T}$ followed by even (odd) $\mathcal{R}$ rotations for $\gamma_1 > 0$ ($\gamma_1 < 0$). The p-SSB$_\pm$ phases are detected, respectively, by the following order parameters:

$$\mathcal{E}_+ = \cos(Q\theta/2), \qquad \mathcal{E}_- = \sin(Q\theta/2). \quad (10)$$

There is no way to identify the residual symmetries of the vacua of one phase with subsets of those of the other, and therefore the phases are distinct and Landau-incompatible. We see the advertised direct transition between them along $\gamma_1 = 0$ for a range of temperatures with continuous critical exponents described by the Gaussian conformal field theory that Eq. (4) flows to.

For odd Q on the other hand, the residual symmetries for both p-SSB$_\pm$ are identical and detected by the same order parameter,

$$\mathcal{O} = \cos((Q-1)\theta/2). \quad (11)$$

The vacua on both sides can be identified as follows:

$$\mathcal{I}\left(\vartheta^+_{n+\frac{Q+1}{2}}\right) = \mathcal{I}(\vartheta_n^-) \Rightarrow \vartheta^+_{n+\frac{Q+1}{2}} \cong \vartheta_n^-. \quad (12)$$

We conclude that both belong to the same phase and that there should exist a path where the vacua $\vartheta^+_{n+[(Q+1)/2]}$ and ϑ_n^- can be smoothly connected without encountering a phase transition. Examples of explicit paths that connect the two regions are sketched in the end matter. Thus, for odd Q, the critical line along $\gamma_1 = 0$ represents "unnecessary criticality" [14,15], which does not correspond to a genuine transition separating distinct phases but is nevertheless stable and reached by tuning a single relevant parameter. To the best of our knowledge all known instances of unnecessary criticality [14,15,39–42] have been observed in quantum mechanical systems [43–45], and ours is the first example in a classical SSB setting.

For completeness, let us consider the remaining phases and transitions in Fig. 1. The full symmetry breaking phase (f-SSB) appears when $\cos(2Q\theta)$ becomes relevant along the $\gamma_1 = 0$ line at low temperatures. This is detected by the order parameter

$$\mathcal{F} = \sin(Q\theta) \quad (13)$$

and has $2Q$ vacua that break all symmetries. The transition between p-SSB$_\pm$ and f-SSB is Landau-compatible and, when continuous, belongs to the Ising universality class [16,33]. Finally, at large T all symmetries are restored when $\cos(\phi)$ becomes relevant along the $\gamma_1 = 0$ line to produce a disordered paramagnet (PM). For $Q \leq 4$, this transition is direct and also Landau-compatible; the universality class depends on Q [16,32].

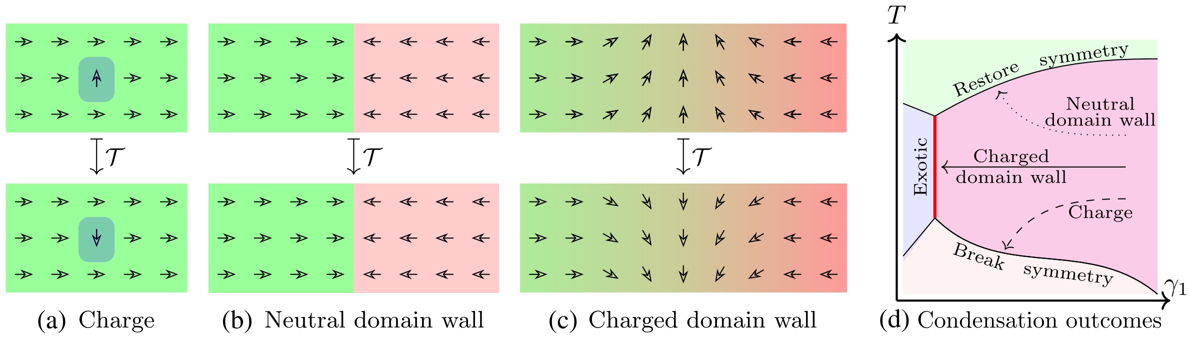

FIG. 2. Schematic representation of various excitations in the p-SSB$_+$ phase and their symmetry transformation. (a) local charges and (b), (c) neutral and charged domain walls, respectively. The latter can be regarded as a bound state of the former two. The transition triggered by condensing each excitation is shown in (d). The neutral domain wall does not carry symmetry charges and its proliferation restores all symmetries, whereas condensing the charge breaks all symmetries. Melting the charged domain walls produces the exotic transitions discussed in this Letter: Landau-incompatible transitions for even Q, which breaks some symmetries while restoring others, and unnecessary criticality for odd Q.

Enhanced symmetries, charged defects—We now study two prominent aspects of DQC transitions in our classical models. The first is the appearance of enhanced symmetries [4] involving rotations between order parameters of the two Landau-incompatible phases that the DQC line separates. This is readily seen for our model. For even Q, we can use the order parameters of p-SSB$_\pm$ phases shown in Eq. (10) to define the two-component unit vector

$$\hat{n} = \big(\mathcal{E}_+, \mathcal{E}_-\big) = \big(\cos(Q\theta/2), \sin(Q\theta/2)\big). \quad (14)$$

Along the direct Landau-incompatible transition, the D_{2Q} symmetry of the JKKN model is enhanced to the $O(2)$ symmetry of the XY model whose order parameter is $\hat{n}$. This is generated by a full θ rotation that transforms the two components of $\hat{n}$, $\mathcal{E}_\pm$ into each other.

The second aspect is the physical picture for the onset of DQC being the proliferation of charged defects that prevents the restoration of symmetries [4]. This is also clearly seen in our model. In the vicinity of the DQC transition along $\gamma_1 = 0$, the relevant excitations are smooth interpolations between vacua with the same residual symmetries. The domain walls resulting from this interpolation are charged under the residual $\mathbb{Z}_2$ symmetry. For illustration, let us focus on $\gamma_1 > 0$ where, for even Q, two of the vacua of the resulting p-SSB$_+$ phase are $\langle\theta_j\rangle = 0$ and π with the same residual symmetry, $\mathbb{Z}_2^{[0]} = \{1, \mathcal{T}\}$. If we create a smooth interpolation between these vacua as shown in Fig. 2(c), we see that the resulting domain wall transforms under $\mathcal{T}$ and thus carries charge. Furthermore, by evaluating the order parameter $\mathcal{E}_+$ on this configuration, we see that it vanishes on the domain wall, whereas the order parameter $\mathcal{E}_-$, which vanishes everywhere else, becomes nonzero at the domain wall. Thus, upon melting the p-SSB$_+$ domain walls, we get p-SSB$_-$ order!.

Experimental realizations—An outstanding challenge for DQC is the relative paucity of experimental platforms for its validation [4]. The results presented in this Letter open up avenues in classical systems where Landau-incompatible transitions can be studied more easily. In fact, they have already been observed in several existing experimental systems [46–55]. For example, the $Q = 4$ model of Eq. (1) describes the adsorption of hydrogen on the (100) surface of tungsten [47,48]. This system exhibits a structural transition [49,50] that is nothing but the Landau-incompatible transition shown in Fig. 1(c). The same model also describes ultrathin deposits of iron on gold substrate [51–54].

Quantum models—All important parts of the phase diagrams of Eq. (1) are qualitatively reproduced by the ground states of the quantum Hamiltonian

$$H = -H_{\mathrm{XXZ}} - hH_0 - \sum_{\ell=1,2,\ldots} \gamma_\ell H_{\ell Q}$$

$$\text{where}, H_{\mathrm{XXZ}} = \sum_j (S_j^x S_{j+1}^x + S_j^y S_{j+1}^y + \Delta S_j^z S_{j+1}^z),$$

$$H_{\ell Q} = \sum_j \left(\prod_{l=0}^{\ell Q-1} S_{j+l}^+ + \prod_{l=0}^{\ell Q-1} S_{j+l}^- \right), \text{ and}$$

$$H_0 = \sum_j (-1)^j S_j^z \text{ or } \sum_j (-1)^j (S_j^x S_{j+1}^x + S_j^y S_{j+1}^y). \quad (15)$$

$\vec{S} = \frac{1}{2}\vec{\sigma}$ are standard spin half angular momentum operators, H_{XXZ} is the XXZ spin chain and H_Q is a term that favors SSB. Both choices of H_0 favor disordered paramagnets that preserve all symmetries, but the second choice also produces a symmetry-protected topological phase for one of the signs of h [35]. The symmetries in Eq. (2) are generated by $\mathcal{R} = \prod_j \exp[(2\pi i/Q)S_j^z]$, $\mathcal{T}$ is a time-reversal symmetry generated by complex conjugation in the Z basis, and the local order parameters corresponding to Eqs. (10), (11), and (13) are

$$\mathcal{E}_\pm = \mathcal{P}_\pm(Q/2), \quad \mathcal{O} = \mathcal{P}_+[(Q-1)/2], \quad \mathcal{F} = \mathcal{P}_-(Q),$$

$$\text{where, } \mathcal{P}_\pm(M) \equiv e^{\frac{i\pi(1\mp1)}{4}}\left(\prod_{l=0}^{M-1} S_{j+l}^+ \pm \prod_{l=0}^{M-1} S_{j+l}^-\right). \tag{16}$$

This model can be bosonized to get the same field theory as in Eq. (4) for $|\Delta| < 1$, up to renormalization of coupling constants.

The role of anomalies—The p-SSB$_\pm$ phases have two more distinct type of excitations. The first are charges shown in Fig. 2(a) corresponding to local deviations from the $\gamma_1 \cos(Q\theta)$ minima, whose condensation further breaks symmetries and produces the transition to the f-SSB phase. The second are "hard" domain walls shown in Fig. 2(b) that do not transform under the residual symmetries and are favored at large values of $|\gamma_1|$. Proliferating these by increasing temperature restores all symmetries and drives the transition to the disordered PM. For small $|\gamma_1|$, charges are bound to neutral domain walls to produce the soft domain walls shown in Fig. 2(c). As $\gamma_1 \to 0$, these bound states, rather than their constituents, melt to drive the Landau-incompatible transitions studied in this Letter.

In several models exhibiting DQC [2,5,7], the binding of charges to defects occurs kinematically due to the *anomalous* nature of underlying microscopic symmetries [4–7]. Anomalies are exotic symmetry representations found in systems constrained by Lieb-Schultz-Mattis conditions [3,56–58] or on the boundaries of symmetry-protected topological phases [7,59]. They forbid strictly on-site representations [59], present an obstruction to gauging [60,61], and disallow a trivial symmetry-preserving phase [12,58]. The latter feature is reflected in the absence of neutral defects that can proliferate to form a trivial phase and permitting only charged ones that can condense to produce DQC [4].

All microscopic symmetries in Eq. (2) are anomaly-free. This is verified by the presence of the symmetry-allowed operator $\cos(\phi)$ in Eq. (4) that produces a trivial phase—a sufficient condition for the absence of anomalies. What we have in our model is arguably a more pedestrian route for the binding of charges to defects—such a bound state may find itself energetically more favorable [62]. However, when $\cos(\phi)$ is irrelevant, a new continuous ϕ rotation symmetry emerges that is preserved by all remaining relevant operators [65], which has a mixed anomaly with the microscopic $\mathcal{R}$ symmetry [12,61]. This microscopic-emergent mixed anomaly may be said to stabilize the Landau-incompatible and unnecessary critical transitions. It is unclear if this is a necessary precondition.

Outlook—We have investigated classical 2D statistical mechanical models hosting stable Landau-incompatible transitions and unnecessary criticality. These transitions are driven by the melting of charged defects and stabilized by a mixed anomaly between microscopic and emergent symmetries unbroken by relevant operators despite all microscopic symmetries being anomaly-free.

Our Letter opens several lines of future investigation. An obvious one is whether we can find other classical models that exhibit similar phenomena [67], especially in higher dimensions. The archetype DQC transition between Néel to valence-bond-solid phases [2] has recently been shown to be first order in nature [69] and it would be interesting to find alternative, classical settings where a Landau-incompatible transition can be present between other phases. For odd Q models, it would be interesting to see how the unnecessary critical surface terminates. In [15,70], it was argued that unnecessary criticality in quantum models is stabilized by the encircling states forming a nontrivial *family* [71–73]. We expect this to be true for our classical model and it would be most interesting to explore this connection further. It would also be useful to further clarify if the stable mixed microscopic-emergent anomaly is a necessary condition for the exotic transitions studied here.

We have shown that exotic transitions can exist under relatively ordinary conditions within reach of existing experiments. It would be gratifying to validate this in more experimental setups. Finally, it would be illuminating to explore what other phenomena attributed to quantum fluctuations can have a classical origin.

Acknowledgments—The authors thank Ruben Verresen, Ryan Thorngren, Steve Simon, Paul Fendley, Sounak Biswas, Yuchi He, and Saranesh Prembabu for useful discussions and the anonymous referees for insightful comments. A. P. was supported by the European Research Council under the European Union Horizon 2020 Research and Innovation Programme, Grant Agreement No. 804213-TMCS.

[1] D. J. Gross, The role of symmetry in fundamental physics, Proc. Natl. Acad. Sci. U.S.A. **93**, 14256 (1996).
[2] T. Senthil, A. Vishwanath, L. Balents, S. Sachdev, and M. P. A. Fisher, Deconfined quantum critical points, Science **303**, 1490 (2004).
[3] E. Lieb, T. Schultz, and D. Mattis, Two soluble models of an antiferromagnetic chain, Ann. Phys. (N.Y.) **16**, 407 (1961).
[4] T. Senthil, Deconfined quantum critical points: A review, in *50 Years of the Renormalization Group* (World Scientific, Singapore, 2024), Chapter 14, pp. 169–195, 10.1142/9789811282386_0014.
[5] B. Roberts, S. Jiang, and O. I. Motrunich, Deconfined quantum critical point in one dimension, Phys. Rev. B **99**, 165143 (2019).
[6] C. Mudry, A. Furusaki, T. Morimoto, and T. Hikihara, Quantum phase transitions beyond Landau-Ginzburg theory

in one-dimensional space revisited, Phys. Rev. B **99**, 205153 (2019).

[7] C. Zhang and M. Levin, Exactly solvable model for a deconfined quantum critical point in 1D, Phys. Rev. Lett. **130**, 026801 (2023).

[8] A. Chatterjee and X.-G. Wen, Symmetry as a shadow of topological order and a derivation of topological holographic principle, Phys. Rev. B **107**, 155136 (2023).

[9] T. Senthil and M. P. A. Fisher, Competing orders, nonlinear sigma models, and topological terms in quantum magnets, Phys. Rev. B **74**, 064405 (2006).

[10] R. R. P. Singh, Does quantum mechanics play a role in critical phenomena?, Physics **3**, 35 (2010).

[11] C. Wang, A. Nahum, M. A. Metlitski, C. Xu, and T. Senthil, Deconfined quantum critical points: Symmetries and dualities, Phys. Rev. X **7**, 031051 (2017).

[12] M. A. Metlitski and R. Thorngren, Intrinsic and emergent anomalies at deconfined critical points, Phys. Rev. B **98**, 085140 (2018).

[13] J. V. José, L. P. Kadanoff, S. Kirkpatrick, and D. R. Nelson, Renormalization, vortices, and symmetry-breaking perturbations in the two-dimensional planar model, Phys. Rev. B **16**, 1217 (1977).

[14] Z. Bi and T. Senthil, Adventure in topological phase transitions in $3+1-$D: Non-Abelian deconfined quantum criticalities and a possible duality, Phys. Rev. X **9**, 021034 (2019).

[15] A. Prakash, M. Fava, and S. A. Parameswaran, Multiversality and unnecessary criticality in one dimension, Phys. Rev. Lett. **130**, 256401 (2023).

[16] See Supplemental Material at http://link.aps.org/supplemental/10.1103/PhysRevLett.134.097103 for further information, including discussion of the phase diagrams and comments on anomalies, which includes Refs. [17–31].

[17] F. Haldane, Demonstration of the Luttinger liquid character of Bethe-ansatz-soluble models of 1-D quantum fluids, Phys. Lett. **81A**, 153 (1981).

[18] R. Dijkgraaf, E. Verlinde, and H. Verlinde, $C=1$ conformal field theories on Riemann surfaces, Commun. Math. Phys. **115**, 649 (1988).

[19] J. Ashkin and E. Teller, Statistics of two-dimensional lattices with four components, Phys. Rev. **64**, 178 (1943).

[20] C.-M. Jian, Z. Bi, and C. Xu, Lieb-Schultz-Mattis theorem and its generalizations from the perspective of the symmetry-protected topological phase, Phys. Rev. B **97**, 054412 (2018).

[21] G. Y. Cho, C.-T. Hsieh, and S. Ryu, Anomaly manifestation of Lieb-Schultz-Mattis theorem and topological phases, Phys. Rev. B **96**, 195105 (2017).

[22] D. V. Else and R. Thorngren, Topological theory of Lieb-Schultz-Mattis theorems in quantum spin systems, Phys. Rev. B **101**, 224437 (2020).

[23] H. C. Po, H. Watanabe, C.-M. Jian, and M. P. Zaletel, Lattice homotopy constraints on phases of quantum magnets, Phys. Rev. Lett. **119**, 127202 (2017).

[24] M. Cheng and N. Seiberg, Lieb-Schultz-Mattis, Luttinger, and 't Hooft—anomaly matching in lattice systems, SciPost Phys. **15**, 051 (2023).

[25] S. Pujari, K. Damle, and F. Alet, Néel-state to valence-bond-solid transition on the honeycomb lattice: Evidence for deconfined criticality, Phys. Rev. Lett. **111**, 087203 (2013).

[26] Z. Zhou, L. Hu, W. Zhu, and Y.-C. He, The SO(5) deconfined phase transition under the fuzzy sphere microscope: Approximate conformal symmetry, pseudo-criticality, and operator spectrum, arXiv:2306.16435.

[27] S. Sachdev, *Quantum Phase Transitions* (Cambridge University Press, Cambridge, England, 2009).

[28] R. J. Baxter, *Exactly Solved Models in Statistical Mechanics* (Academic Press, New York, 1982).

[29] F. Franchini, *An Introduction to Integrable Techniques for One-Dimensional Quantum Systems* (Springer International Publishing, New York, 2017).

[30] J. T. Chalker, *Spin liquids and frustrated magnetism, Topological Aspects of Condensed Matter Physics*, edited by C. Chamon, Mark O. Goerbig, R. Moessner, and Leticia F. Cugliandolo (Oxford University Press, 2017), p. 123, 10.1093/acprof:oso/9780198785781.003.0003.

[31] R. Kenyon, An introduction to the dimer model, arXiv:math/0310326.

[32] P. Lecheminant, A. O. Gogolin, and A. A. Nersesyan, Criticality in self-dual sine-Gordon models, Nucl. Phys. **B639**, 502 (2002).

[33] G. Delfino and G. Mussardo, Non-integrable aspects of the multi-frequency Sine-Gordon model, Nucl. Phys. **B516**, 675 (1998).

[34] R. Verresen, R. Thorngren, N. G. Jones, and F. Pollmann, Gapless topological phases and symmetry-enriched quantum criticality, Phys. Rev. X **11**, 041059 (2021).

[35] S. Mondal, A. Agarwala, T. Mishra, and A. Prakash, Symmetry-enriched criticality in a coupled spin ladder, Phys. Rev. B **108**, 245135 (2023).

[36] J. Villain, Theory of one-and two-dimensional magnets with an easy magnetization plane. II. The planar, classical, two-dimensional magnet, J. Phys. **36**, 581 (1975).

[37] P. H. Ginsparg, Applied conformal field theory, in *Les Houches Summer School in Theoretical Physics: Fields, Strings, Critical Phenomena* (North-Holland, 1988), arXiv:hep-th/9108028.

[38] P. Di Francesco, P. Mathieu, and D. Senechal, *Conformal Field Theory*, Graduate Texts in Contemporary Physics (Springer-Verlag, New York, 1997).

[39] F. Anfuso and A. Rosch, String order and adiabatic continuity of Haldane chains and band insulators, Phys. Rev. B **75**, 144420 (2007).

[40] S. Moudgalya and F. Pollmann, Fragility of symmetry-protected topological order on a Hubbard ladder, Phys. Rev. B **91**, 155128 (2015).

[41] R. Verresen, J. Bibo, and F. Pollmann, Quotient symmetry protected topological phenomena, arXiv:2102.08967.

[42] Y. He, D. M. Kennes, C. Karrasch, and R. Rausch, Terminable transitions in a topological fermionic ladder, Phys. Rev. Lett. **132**, 136501 (2024).

[43] J. Wang, X.-G. Wen, and E. Witten, Symmetric gapped interfaces of SPT and SET states: Systematic constructions, Phys. Rev. X **8**, 031048 (2018).

[44] A. Prakash, J. Wang, and T.-C. Wei, Unwinding short-range entanglement, Phys. Rev. B **98**, 125108 (2018).

[45] A. Prakash and J. Wang, Unwinding fermionic symmetry-protected topological phases: Supersymmetry extension, Phys. Rev. B **103**, 085130 (2021).
[46] J. M. Kosterlitz, Kosterlitz–Thouless physics: A review of key issues, Rep. Prog. Phys. **79**, 026001 (2016).
[47] K. Kankaala, T. Ala-Nissila, and S.-C. Ying, Theory of adsorbate-induced surface reconstruction on w(100), Phys. Rev. B **47**, 2333 (1993).
[48] T. Ala-Nissila, E. Granato, K. Kankaala, J. M. Kosterlitz, and S.-C. Ying, Numerical studies of the two-dimensional xy model with symmetry-breaking fields, Phys. Rev. B **50**, 12692 (1994).
[49] J. J. Arrecis, Y. J. Chabal, and S. B. Christman, H-induced structural phase transitions on w(100) by surface infrared spectroscopy, Phys. Rev. B **33**, 7906 (1986).
[50] K. Griffiths, D. A. King, and G. Thomas, Hydrogen-induced symmetry switching of the w001 $(\sqrt{2}\times\sqrt{2})\,r45°$ low temperature phase, Vacuum **31**, 671 (1981).
[51] C. Rau and M. Robert, Anisotropic XY model for two-dimensional Fe, Mod. Phys. Lett. B **10**, 223 (1996).
[52] L. D. Roelofs, Order in two dimensions, Appl. Surf. Sci. **11–12**, 425 (1982).
[53] W. Dürr, M. Taborelli, O. Paul, R. Germar, W. Gudat, D. Pescia, and M. Landolt, Magnetic phase transition in two-dimensional ultrathin Fe films on Au(100), Phys. Rev. Lett. **62**, 206 (1989).
[54] C. Rau, C. Jin, and G. Xing, Monolayer-ferromagnetism, critical behavior and anisotropies of Fe(100)/Au(100), Fe (100)/Ag(100) and Tb/Fe(100)/Ag(100) films, Phys. Lett. A **144**, 406 (1990).
[55] T. E. Felter, R. A. Barker, and P. J. Estrup, Phase transition on mo(100) and w(100) surfaces, Phys. Rev. Lett. **38**, 1138 (1977).
[56] M. B. Hastings, Lieb-Schultz-Mattis in higher dimensions, Phys. Rev. B **69**, 104431 (2004).
[57] M. Oshikawa, Commensurability, excitation gap, and topology in quantum many-particle systems on a periodic lattice, Phys. Rev. Lett. **84**, 1535 (2000).
[58] A. Prakash, An elementary proof of 1D LSM theorems, arXiv:2002.11176.
[59] D. V. Else and C. Nayak, Classifying symmetry-protected topological phases through the anomalous action of the symmetry on the edge, Phys. Rev. B **90**, 235137 (2014).
[60] X.-G. Wen, Classifying gauge anomalies through symmetry-protected trivial orders and classifying gravitational anomalies through topological orders, Phys. Rev. D **88**, 045013 (2013).
[61] E. Fradkin, *Quantum Field Theory: An Integrated Approach* (Princeton University Press, Princeton, NJ, 2021).
[62] An analogous charge-binding transition and associated exotic critical phenomena in a 2d classical model were investigated in Refs. [63,64].
[63] Y. Shi, A. Lamacraft, and P. Fendley, Boson pairing and unusual criticality in a generalized XY model, Phys. Rev. Lett. **107**, 240601 (2011).
[64] P. Serna, J. T. Chalker, and P. Fendley, Deconfinement transitions in a generalised XY model, J. Phys. A **50**, 424003 (2017).
[65] The critical Ising model, which is the archetypal Landau-compatible transition, also has a mixed anomaly between the microscopic Ising symmetry and the emergent Kramers-Wannier symmetry [66]. The key difference is that this mixed anomaly is explicitly broken by *relevant* operators, whereas the same is broken by *irrelevant* operators in our model.
[66] C. Zhang and C. Córdova, Anomalies of $(1+1)D$ categorical symmetries, arXiv:2304.01262.
[67] Numerical evidence for a direct Landau-incompatible transition in an alternative classical model was presented in Ref. [68].
[68] A. Chatterjee and X.-G. Wen, Holographic theory for continuous phase transitions: Emergence and symmetry protection of gaplessness, Phys. Rev. B **108**, 075105 (2023).
[69] J. Takahashi, H. Shao, B. Zhao, W. Guo, and A. W. Sandvik, SO(5) multicriticality in two-dimensional quantum magnets, arXiv:2405.06607.
[70] A. Prakash and S. A. Parameswaran, Charge pumps, boundary modes, and the necessity of unnecessary criticality, arXiv:2408.15351.
[71] A. Kitaev, Differential forms on the space of statistical mechanics models, *Talk at the Conference in Celebration of Dan Freed's 60th Birthday* (2019), https://web.ma.utexas.edu/topqft/talkslides/kitaev.pdf.
[72] P.-S. Hsin, A. Kapustin, and R. Thorngren, Berry phase in quantum field theory: Diabolical points and boundary phenomena, Phys. Rev. B **102**, 245113 (2020).
[73] X. Wen, M. Qi, A. Beaudry, J. Moreno, M. J. Pflaum, D. Spiegel, A. Vishwanath, and M. Hermele, Flow of higher Berry curvature and bulk-boundary correspondence in parametrized quantum systems, Phys. Rev. B **108**, 125147 (2023).
[74] The identification by conjugation is often not stated in literature [75]. However, it is important for correct classification, and without it we would overcount the number of SSB phases. For Abelian groups, conjugation acts trivially, and various subgroups indeed represent distinct phases. For non-Abelian groups, this is not the case.
[75] X. Chen, Z.-C. Gu, and X.-G. Wen, Complete classification of one-dimensional gapped quantum phases in interacting spin systems, Phys. Rev. B **84**, 235128 (2011).
[76] M. Hermele, Families of gapped systems and quantum pumps, Talk at Center for Mathematical Sciences and Applications (2021), www.youtube.com/watch?v=wtaC0tqXZMU.

End Matter

Spontaneous symmetry breaking and Landau compatibility—We present a discussion of spontaneous symmetry breaking (SSB) and Landau compatibility. For simplicity, we will assume that we are working with a classical statistical mechanical system whose symmetries $g\in G$ form a finite group of order $|G|$.

Classifying SSB phases: A system is said to be in an SSB phase if it has multiple vacua that are not invariant under the full set of symmetries. For a given vacuum v_α, let us denote by $H_\alpha \subset G$ the subgroup of residual symmetries that leaves it invariant. The set of symmetries in G, but not in H_α, denoted $G\backslash H_\alpha$, transform the vacuum v_α to other vacua v_β, although several elements of $G\backslash H_\alpha$ can give the same v_β. It is straightforward to see that the set of unique transformations are labeled by the cosets of H_α and starting with v_α, the number of distinct vacua we can reach this way is given by the index $[G{:}H_\alpha]$. If $g_{\alpha\beta}$ takes $v_\alpha \to v_\beta$, the residual symmetry group of v_β is $H_\beta = g_{\alpha\beta} H_\alpha g_{\alpha\beta}^{-1}$. The cosets of H_α and H_β are identical. Thus, the generated $[G{:}H_\alpha]$ vacua family would be the same, independent of the initial choice of v_α. We conclude that given a system with symmetry G, distinct SSB phases are labeled by distinct families of conjugate subgroups [74].

For a finite group G, the different SSB phases are nicely organized by the lattice of conjugate subgroups and visualized by a Hasse diagram where the families of conjugate subgroups are connected by the presence of an inclusion map, i.e., when one family is a subgroup of the other. In Fig. 3, we have shown this for the dihedral symmetries $D_{2Q} \cong \mathbb{Z}_Q \rtimes \mathbb{Z}_2$ considered in the main text for $Q = 2, 4$, with the presentation

$$D_{2Q} = \langle \mathcal{R}, \mathcal{T} | \mathcal{R}^Q = \mathcal{T}^2 = 1, \mathcal{R}\mathcal{T} = \mathcal{T}\mathcal{R}^{-1} \rangle. \tag{A1}$$

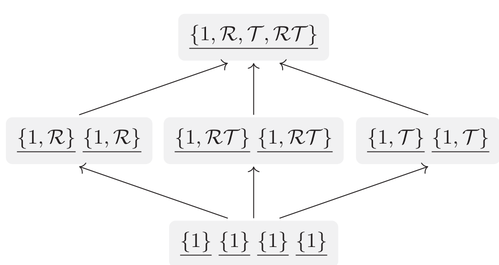

(a) $G = D_4 \cong \mathbb{Z}_2 \times \mathbb{Z}_2$

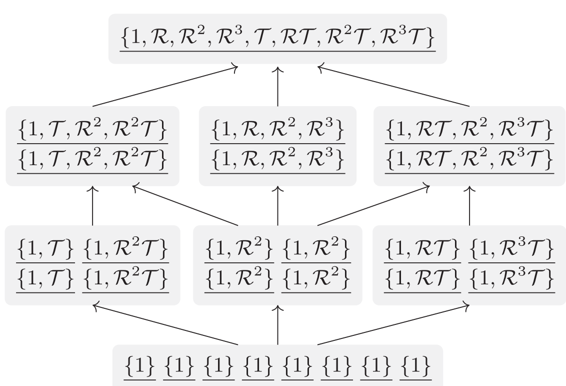

(b) $G = D_8 \cong \mathbb{Z}_4 \rtimes \mathbb{Z}_2$

FIG. 3. Hasse diagram of the lattice of conjugate subgroups for the (a) Abelian $D_4 \cong \mathbb{Z}_2 \times \mathbb{Z}_2$ and (b) non-Abelian $D_8 \cong \mathbb{Z}_4 \rtimes \mathbb{Z}_2$ groups. The arrows represent an inclusion map, and two entries connected by a sequence of maps represent Landau-compatible phases. Horizontal lines represent the various vacua over which their residual symmetries are listed. We see that the phase with all symmetries broken (bottom) and all symmetries preserved (top) are Landau-compatible with all other phases.

Landau compatibility: We can distinguish between Landau-compatible and Landau-incompatible transitions using the lattice of conjugate subgroups and its Hasse diagram. Two SSB phases represented by two families of conjugate subgroups are Landau-compatible if they are connected in the Hasse diagram by the composition of a sequence of arrows. Physically, we can understand this as follows: if we place ourselves in one of the vacua of the SSB phase with residual symmetries $H_\alpha \subset G$, we can treat it as a stand-alone system with symmetries H_α. These can be spontaneously broken into a conjugate family of subgroups $K_{\alpha\beta} \subset H_\alpha$. All other transitions are Landau-incompatible. Physically, a transition between Landau-incompatible phases cannot be understood by a hierarchical splitting of each vacuum, but rather by a more drastic process involving multiple vacua coming together and reorganizing themselves.

In particular the fully symmetric phase with unique vacuum and fully broken phase with $|G|$ vacua are Landau-compatible with all SSB phases. The interesting cases are the phases with partial symmetry breaking as we saw in the main text. Landau-compatible transitions are characterized by a change in the number of vacua (although this change does not guarantee compatibility). Moreover, Landau-incompatible transitions can occur between two SSB phases with the same number of vacua, as seen in the main text.

Explicit paths avoiding the unnecessary critical surface for odd Q—In the main text, it was argued using symmetry that, for odd Q, the p-SSB$_\pm$ regions belong to the same phase and can be connected without encountering any phase transitions or violating any symmetries. Here, we construct explicit such paths inspired by the so-called domain-wall pump [76].

Bipartite lattice: First, we consider a path, schematically shown in Fig. 4, that works on bipartite lattices within an extended family of Hamiltonians of the form

$$H = -\sum_{\langle j,k \rangle} J_1 \cos(\theta_j - \theta_k) - \sum_{\langle\langle j,k \rangle\rangle} J_2[j] \cos(\theta_j - \theta_k) - \sum_{\ell=1,2,\ldots} \sum_j \gamma_\ell[j] \cos(\ell Q \theta_j). \tag{B1}$$

Equation (B1) contains nearest neighbor $\langle j,k \rangle$ and next nearest neighbor $\langle\langle j,k \rangle\rangle$ XY couplings that are allowed to differ on the two sublattices, which we label as red and

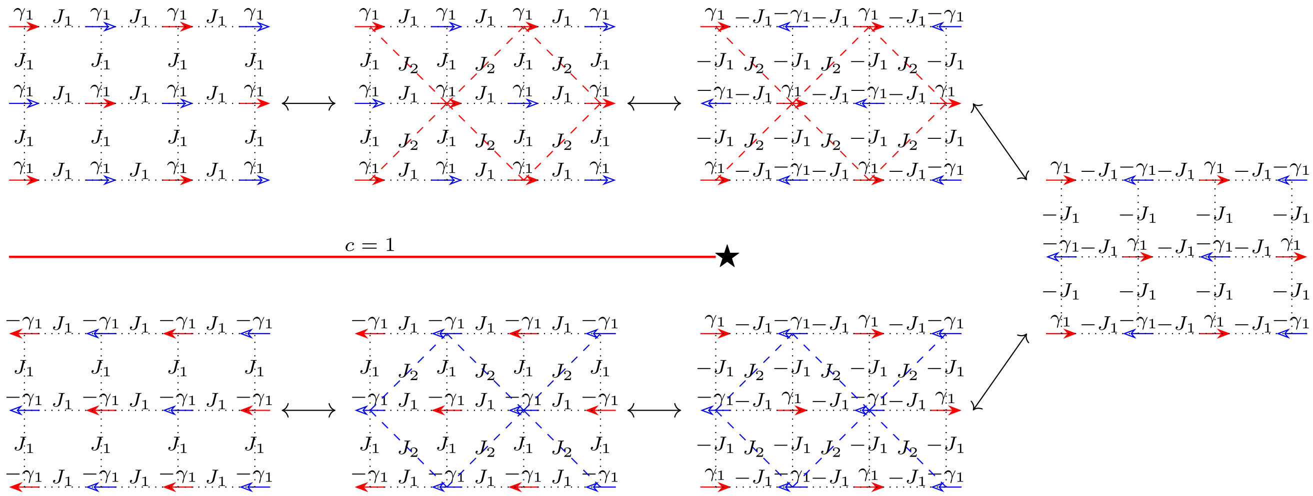

FIG. 4. A path for bipartite lattices avoiding the unnecessary critical surface (denoted by $c = 1$). We expect this surface to abruptly terminate.

blue. For our path, we begin with $\gamma_1 > 0$ in the p-SSB$_+$ region in one of its vacua, e.g., $\langle\theta_j\rangle = 0$ as shown in Fig. 4. We want to flip the sign of γ_1 without encountering a phase transition. To achieve this, we first introduce a large $J_2 \gg J_1$ coupling only on the red sublattice, which preserves the vacuum. We then flip the on-site anisotropy $\gamma_1 \to -\gamma_1$ on the blue sublattice as well as all $J_1 \to -J_1$; following which we remove the red $J_2 \to 0$. This produces an antiferromagnetic alignment between neighboring spins and favors $\langle\theta_j\rangle = \pi$ on the blue spins. We then repeat the same steps for the other sublattice as shown in Fig. 4. In the end, we obtain Eq. (B1) with γ_1 reversed and $\langle\theta_j\rangle = \pi$ on all spins, landing us on p-SSB$_-$.

At each step of this symmetry-preserving path, we did not change the number of vacua. The magnitude of the order parameter detecting the p-SSB$_\pm$ phases, $\mathcal{O}$ defined in Eq. (11), has a nonvanishing average xthroughout the path, although its sign develops a spatial variation.

Any lattice: An unnecessary criticality avoiding path can be obtained for any lattice by nucleating a domain and sweeping it across the entire lattice as shown in Fig. 5. A domain is enclosed by a path on the dual lattice by flipping all anisotropies, $\gamma_1 \mapsto -\gamma_1$, within and $J_1 \mapsto -J_1$ on the domain wall as shown in Fig. 5. Alternatively, instead of a single location, domains can be nucleated on various well-separated locations, grown, and merged.

For odd Q, the above paths does not risk a phase transition as the process of producing γ_1 of different signs between neighboring spins $\langle j,k\rangle$ does not frustrate flipping the J_1 connecting them—both favor a spin mismatch of $\theta_j - \theta_k = \pi$. This is not true for even Q.

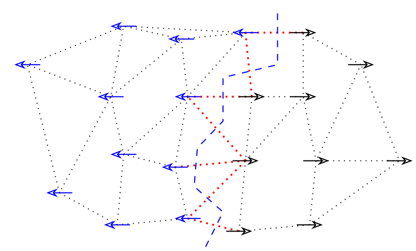

FIG. 5. Sweeping a domain across the lattice transforms between p-SSB$_\pm$ without any phase transitions.